Available online at www.sciencedirect.com
SCIENCE DIRECT
Polymer 46 (2005) 3708–3719
polymer
www.elsevier.com/locate/polymer

Coupling between mass diffusion and film temperature evolution in gravimetric experiments

F. Doumenc*, B. Guerrier, C. Allain

Lab. FAST (Université Pierre et Marie Curie – Université Paris Sud – CNRS), Bât. 502, Campus Universitaire, 91405 Orsay, France

Received 13 May 2004; received in revised form 13 December 2004; accepted 14 February 2005
Available online 31 March 2005

Abstract

In gravimetric experiments, the swelling and the drying of polymer films is used to investigate the thermodynamic properties and the mutual diffusion coefficient of polymer/solvent systems. Usually thermodynamic equilibrium at the interface between the film and the solvent vapor and thermal equilibrium between the film and the surroundings are assumed. In this paper we show that the second assumption may fail. Indeed, during a swelling or drying experiment, the temperature of the film surface changes due to the latent heat of vaporization, which induces a variation of the activity. When the corresponding variation of the solvent content is of the same order than the variation due to the sorption experiment and when the thermal time constant is significant compared to the characteristic mass diffusion time, this thermal effect must be taken into account when analyzing sorption data. We evaluate the consequence of this thermal effect on gravimetric experiments and develop a complete model to take this phenomenon into account when analyzing sorption data. As an example, the mutual diffusion coefficient for the system PIB (polyisobutylene)/toluene is estimated for various solvent concentrations at 25 °C.

Keywords: Gravimetry; Mutual diffusion; PIB (polyisobutylene)

1. Introduction

Studying the swelling and the drying of polymer films in a controlled vapor of solvent is a useful method to investigate the thermodynamic properties and the mutual diffusion coefficient of polymer/solvent systems. The solvent concentration in the film is often measured by weighing (gravimetric methods). During a swelling or drying experiment, the temperature of the film surface changes due to the latent heat of vaporization, so that the film is no more in thermal equilibrium with the surroundings. This thermal effect is generally neglected. However, this assumption may fail. Indeed the variation of temperature due to vaporization or condensation induces a small variation of the activity. In some cases, the corresponding variation of the solvent volume fraction can be of the same order than the solvent change during the sorption experiment. If the thermal time constant is significant compared to the characteristic mass diffusion time, this thermal effect must be taken into account when analyzing sorption data. The present paper thoroughly analyzes this thermal effect and characterizes the experimental conditions of appearance.

Experimental set-ups consist of an accurate balance coupled with a chamber whose temperature and pressure are controlled. The sample is located in the chamber and changes in the solvent vapor pressure allow the polymer film to swell or dry. In all the results presented in this paper no inert gas is present and the solvent vapor is the only gas present in the chamber, so that the total pressure and the solvent vapor pressure are the same. Indeed when an inert gas is present in the chamber, specific problems occur due to the diffusion time of the solvent vapor in the inert gas [1]. Sorption or desorption experiments consist in performing a vapor pressure step and recording the dynamic response of the film to this pressure step. Analysis of weight evolution versus time gives information on the mutual diffusion coefficient and on relaxation induced phenomena when the system is glassy (for example [2–6]). If the magnitude of the pressure change is small enough (differential step), the

* Corresponding author. Tel.: +33 1 69 15 80 63; fax: +33 1 69 15 80 60.
E-mail address: doumenc@fast.u-psud.fr (F. Doumenc).

0032-3861/$ - see front matter © 2005 Elsevier Ltd. All rights reserved.
doi:10.1016/j.polymer.2005.02.098

Nomenclature (SI Units)

a	solvent activity
c_{al}	substrate heat capacity (J/(kg K))
c_P	polymer heat capacity (J/(kg K))
c_S	solvent heat capacity (J/(kg K))
$\mathcal{C}$	surface heat capacity of the sample (substrate + film) (J/(m^2 K))
D_{SP}	mutual diffusion coefficient (m^2/s)
e	solution thickness (m)
e_0	initial solution thickness (m)
e_{al}	substrate thickness (m)
e_{dry}	dry film thickness (m)
h^{cond}	conductive heat transfer coefficient (W/(m^2 K))
h^{rad}	radiative heat transfer coefficient (W/(m^2 K))
h_{th}	global heat transfer coefficient (W/(m^2 K))
$H(t)$	Heaviside function
L	solution latent heat (J/kg)
M_{dry}	dry mass of the film (kg)
M_W	polymer weight average molecular weight (kg/mol)
P_{VS}	saturated vapor pressure of the solution (Pa)
P_{VS0}	saturated vapor pressure of the solvent (Pa)
P_V	vapor pressure in the chamber (Pa)
R	ratio of the concentration increment at $t=0^+$ to the equilibrium concentration increment (cf. Eq. (10))
S	sample surface (m^2)
T	solution temperature (K)
T_0	initial solution temperature (K)
T_a	chamber temperature (K)
$\bar{V}_S$	solvent specific volume (m^3/kg)
$\bar{V}_{PIB}$	PIB specific volume (m^3/kg)
$\delta(t)$	delta function
ε_{al}	total hemispheric emissivity of the substrate
ε_{film}	total hemispheric emissivity of the film
λ	thermal conductivity of the solvent vapor (W/(m K))
ϕ^{rad}_{film}	film radiation transfer rate (W)
ϕ^{rad}_{al}	substrate radiation transfer rate (W)
ρ_{al}	substrate density (Kg/m^3)
ρ_P	polymer density (Kg/m^3)
ρ_S	solvent density (Kg/m^3)
σ	Stefan–Boltzmann constant (W/(m^2 K^4))
τ_d	characteristic mass diffusion time (s)
τ_{th}	characteristic thermal diffusion time (cf. Eq. (8)) (s)
φ_P	polymer volume fraction (m^3/m^3)
φ_S	solvent volume fraction (m^3/m^3)
φ_{S0}	initial solvent volume fraction (m^3/m^3)
φ^i_S	solvent volume fraction at the solution/vapor interface (m^3/m^3)
Φ_m	solvent evaporation mass flux per unit area (kg/(m^2 s))
χ	Flory–Huggins interaction parameter

solvent concentration is only slightly changed and the mutual diffusion coefficient may be assumed constant during the differential step. With the assumption of thermodynamic equilibrium at the vapor/film interface and the assumption of ideal gas for the solvent vapor, the equality of the solvent chemical potential in the solution and in the vapor leads to the following equation:

$$a = \frac{P_{VS}(\varphi^i_S, T)}{P_{VS0}(T)} \tag{1}$$

where a is the solvent activity, P_{VS0} the saturated pressure vapor of the solvent, P_{VS} the saturated pressure vapor of the solution, φ^i_S the solvent volume fraction in the solution near the interface and T the temperature of the solution.

In the rubbery domain, the Flory–Huggins model gives

$$a = \varphi^i_S \exp[(1-\varphi^i_S) + \chi(1-\varphi^i_S)^2] \tag{2}$$

where χ is the interaction parameter which characterizes the affinity between the solvent and the polymer.

Actually, the two variables that are experimentally controlled are the pressure (P_V) and the temperature (T_a) in the chamber. Given the time scales involved the pressure may always be assumed uniform in the chamber, and changing the pressure set-point in the chamber is then equivalent to change P_{VS}. This is not true for the temperature, since drying or swelling induces a variation of the temperature of the film surface, T, which is no more equal to the temperature of the chamber, T_a. For a fixed P_{VS}, T and φ^i_S are coupled via Eqs. (1) and (2), through the dependence of P_{VS0} on T. The time evolution of φ^i_S towards the new equilibrium value (corresponding to the pressure P_{VS} and temperature T_a) thus depends on the thermal time constant of the system which may be significant. A pressure increment is then not equivalent to an activity increment or to a surface concentration increment as usually assumed when fitting gravimetric experiments. As will be seen in Section 3 this phenomenon is especially strong when the slope of the activity versus solvent volume fraction is small, i.e. at high solvent concentration for polymer solutions. Indeed, a small variation of the activity due to a small variation of T induces a great change of φ^i_S. For some experimental configurations this phenomenon has to be taken into account when fitting sorption kinetics. Moreover, the thermal effect may limit the domain of diffusion coefficient that can be explored by gravimetric experiments. The coupling between mass and temperature evolution during sorption experiments has already been studied for

another system (water+cellulose acetate) by Armstrong and co-authors [7]. In this previous study only free films are considered. In the present paper, we analyze the influence of the thermal characteristics and thickness of the substrate on the magnitude of the thermal effect. Moreover, the equations are presented more formally, especially for the boundary condition at the interface that refers explicitly to the activity of the polymer solution. With such formalism, the influence of the system thermal characteristics and of the solution physicochemical properties is clearly highlighted.

In the present paper quantitative illustrations are given on the system PIB (polyisobutylene)/toluene. Let us notice that it is interesting to get information on the behavior of the mutual diffusion coefficient for the PIB/toluene system since, while used in many studies, only few data are available in the literature.

The paper is organized as follows: the gravimetric set-up and the system are presented in Section 2. Section 3 is devoted to the thermal analysis and highlights the relevant parameters to be taken into account. In Section 4 the mutual diffusion coefficient for the system PIB/toluene is estimated for various solvent concentrations, illustrating the thermal effect.

2. Experimental

2.1. Gravimetric set-up

The gravimetric set-up is a 'Hiden IGA system' based on a precise balance. The sample is hanged in the chamber where temperature and pressure are accurately controlled. Temperature regulation is operated with a fluid circulating in the outer wall of the chamber and coming from a thermostated bath. The temperature is measured by a platinum resistance thermometer (Pt100) located near the sample. Temperature stability is ± 0.05 °C. The chamber is connected through various valves to a vacuum pump on one hand and to a solvent tank on the other hand, where liquid solvent is in equilibrium with its vapor at 55 °C. Pressure is regulated with a PID controler. The pressure stability is better than 2 Pa. The pressure has been varied between 1 Pa and 95% of the saturated vapor pressure of the solvent. The weight measurement noise is about 1 μg and the reproductibility (same measurement performed at various times) about 10 μg. The chamber is a cylinder with diameter 34.5 mm and height 300 mm. All the experiments presented in this paper have been performed for a temperature set-point equal to 25 °C.

2.2. System

The polymer/solvent solution used in this study is PIB/toluene. Two samples of PIB (supplied by ALDRICH) were used, with $M_w = 5\times10^5$ g/mol and 10^6 g/mol and polydispersity 2.5 and 1.7, respectively. Toluene was supplied by Prolabo (Chromatographic use, purity 99.9%). The glass transition temperature of PIB is -76 °C (ALDRICH). The experimental temperature is then far above the glass transition and the system remains rubbery all along the experiments. In such a way no glass transition occurs, the kinetics are easier to analyze and suitable to illustrate the thermal effect under study. Films were prepared by slow drying of PIB/toluene solutions in glass dishes. The film thickness depends on the initial concentration and initial volume of the solution in the dish. Drying is achieved by heating the film at 60 °C for several days. The film is then taken off from the dish and put on an aluminium substrate (38 μm thick for most of the experiments). A disk of diameter 20 mm is cut with a hollow punch. The sample (PIB film+aluminium substrate) is hanged horizontally in the balance chamber and weighed to get the dry mass of the sample. The film thickness is estimated a posteriori, at the end of experiments: The aluminium substrate is cleaned in toluene to dissolve the PIB film and weighed. The PIB mass, M_{dry}, is then deduced by difference and the thickness of the PIB film, e_{dry}, estimated from its mass and from the specific volume of PIB ($\bar{V}_{PIB} = 1.087\times10^{-3}$ m^3/kg).

Equilibrium solvent concentrations in the solution have been obtained for various samples with thicknesses 9, 13, 52, 63 and 67 μm ($M_W = 5\times10^5$ g/mol) and 99 μm ($M_w = 10^6$ g/mol). By 'equilibrium' one means that the solvent concentration may be supposed uniform in the film: $\bar{\varphi}_S = \varphi_S^i$. Experimental points have been obtained by setting a constant pressure in the chamber and waiting until the film weight was constant. Results are summarized in Fig. 1. Relative error on the activity is deduced from the precision

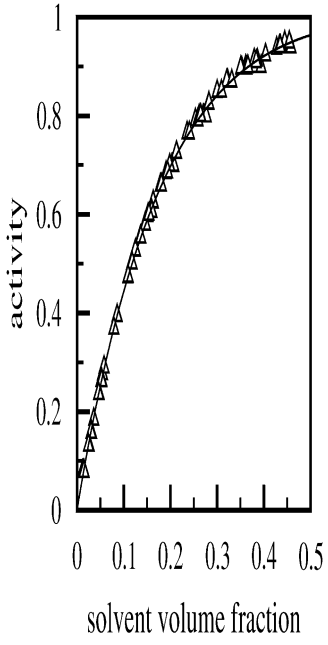

Fig. 1. Activity versus solvent volume fraction for PIB/toluene films [dry film thickness = 9, 13, 52, 63, 67 μm ($M_w = 5\times10^5$ g/mol) and 99 μm ($M_w = 10^6$ g/mol)]. The full line corresponds to the Flory–Huggins model, with $\chi = 0.75 - 0.26\varphi_S$.

of the pressure and temperature measurements: $\Delta a/a = \Delta P_V/P_V + \Delta P_{VS0}/P_{VS0} \leq 10^{-2}$. Relative error on the solvent volume fraction is mainly due to the error on the estimation of the dry mass of the film, M_{dry} : $\Delta\bar{\varphi}_S/\bar{\varphi}_S \simeq 0.1/M_{dry}$ (M_{dry} in mg). As can be seen, the reproducibility is good and the results for different film thicknesses all gather on the same curve. They can be fitted by the Flory–Huggins model (Eq. (2)) with an interaction parameter χ depending on the solvent volume fraction [8,9]: for $\varphi_S < 0.5$, $\chi = 0.75 - 0.26\varphi_S$.

3. Thermal model

3.1. Equations

To understand the role of the thermal effect in gravimetric experiments, a first model is developed in the case of an infinite mutual diffusion coefficient, i.e. the mass diffusion characteristic time inside the film is negligible. With this assumption the solvent volume fraction, $\varphi_S(t)$, is uniform through the film, so that the superscript 'i' denoting the solvent concentration at the interface is omitted in this section.

Given the high thermal diffusivity and conductivity of the aluminium substrate and the small thickness of the PIB/toluene film, the sample (film + aluminium sheet) can be characterized by a unique temperature, $T(t)$. Indeed the thermal diffusion time inside the sample is less than 0.1 s for a 100 μm film and less than 10 s for a 1 mm film. The Biot number [10], which gives the ratio between the variation of temperature in the film and the temperature difference between the film and chamber temperature, is very small (≤ 0.01).

The two external inputs of the system are the pressure in the chamber, $P_V(t)$, and the temperature of the chamber, $T_a(t)$, both imposed by the regulation systems. The unknown variables are $\varphi_S(t)$, $T(t)$ and the film thickness $e(t)$, whose time evolution are derived from the following equations.

With the assumption of thermodynamical equilibrium at the interface, the solvent concentration and the temperature are coupled through the activity, as previously said in the introduction:

$$a = P_{VS}(\varphi_S, T)/P_{VS0}(T) = P_V/P_{VS0}(T) = \varphi_S \exp[(1-\varphi_S) + \chi(1-\varphi_S)^2] \quad (3)$$

Given the weak dependence of the interaction parameter χ with the temperature, the activity may be considered as a function of φ_S only.

The second equation expresses the system heat balance taking into account the energy needed to vaporize the solvent (or brought by the condensation when considering a desorption step), the variation of the internal energy of the sample and the exchange with the environment at temperature T_a:

$$\mathcal{C}\frac{dT}{dt} = h_{th}(T_a - T) - L\Phi_m = h_{th}(T_a - T) + \frac{L}{\bar{V}_S}\frac{d(e\varphi_S)}{dt} \quad (4)$$

where Φ_m is the solvent evaporation mass flux, L is the solution latent heat (nearly identical to the solvent latent heat), $\bar{V}_S$ is the solvent specific volume, e is the solution thickness. h_{th} is the global heat transfer coefficient between the sample and the chamber, that takes into account heat exchanges between the chamber and the upper surface of the sample (polymer film) on one hand and the lower surface (aluminium substrate) on the other hand: $h_{th} = h_{th}^{film} + h_{th}^{al}$. Heat exchanges are mainly due to radiative transfer between the sample and the chamber walls. $\mathcal{C}$ is the heat capacity of the sample:

$$\mathcal{C}(t) = [\rho_{al}c_{al}e_{al} + (\rho_S c_S \varphi_S + \rho_P c_P \varphi_P)e(t)]$$

where ρ_{al}, c_{al} and e_{al} are the density, heat capacity and thickness of the aluminium sheet, ρ_S, c_S and ρ_P, c_P are the density and heat capacity of solvent and polymer, respectively. φ_P is the polymer volume fraction ($\varphi_P = 1 - \varphi_S$).

Writing that the volume is conservative and that the polymer does not evaporate leads to the following equalities:

$$\frac{de}{dt} = -\bar{V}_S\Phi_m = \frac{d(e\varphi_S)}{dt} \quad (5)$$

Initial conditions are:

$$T(t=0) = T_0 = T_a, \quad \varphi_S(t=0) = \varphi_{S0}, \quad e(t=0) = e_0$$

An analytical expression of the time evolution of the sample temperature and solvent concentration in response to a pressure step in the chamber can be derived from linearization of the equations and use of the Laplace transform. The temperature of the chamber, T_a, is kept constant. Details of the calculation are given in Annex A. When submitted to a differential pressure step $\Delta P_V H(t)$, where $H(t)$ is the Heaviside function, the temperature $T(t)$ and solvent volume fraction $\varphi_S(t)$ are:

$$\Delta T(t) = T(t) - T_a = \frac{\xi \Delta P_V}{K_\varphi \tau_{th}}\exp(-t/\tau_{th}) \quad (6)$$

$$\Delta\varphi_S(t) = \varphi_S - \varphi_{S0} = \frac{\Delta P_V}{K_\varphi}\left[H(t) - \frac{K_P\xi}{K_a\tau_{th}}\exp(-t/\tau_{th})\right] \quad (7)$$

with:

$$\xi = \frac{Le_0}{h_{\mathrm{th}}\bar{V}_{\mathrm{S}}(1-\varphi_{\mathrm{S0}})}, \quad K_\varphi = P_{\mathrm{VS0}}(T_0)\left.\frac{\mathrm{d}a}{\mathrm{d}\varphi_{\mathrm{S}}}\right|_{\varphi_{\mathrm{S0}}},$$

$$K_{\mathrm{a}} = \frac{1}{a(\varphi_{\mathrm{S0}})}\left.\frac{\mathrm{d}a}{\mathrm{d}\varphi_{\mathrm{S}}}\right|_{\varphi_{\mathrm{S0}}}, \quad K_{\mathrm{P}} = \frac{1}{P_{\mathrm{VS0}}(T_0)}\left.\frac{\mathrm{d}P_{\mathrm{VS0}}}{\mathrm{d}T}\right|_{T_0},$$

$$\tau_{\mathrm{th}} = \frac{\mathcal{C}_{(t=0)}}{h_{\mathrm{th}}} + \frac{K_{\mathrm{P}}}{K_{\mathrm{a}}}\xi \tag{8}$$

Eq. (7) can be also written in the following way:

$$\Delta\varphi_{\mathrm{S}}(t)/\Delta\varphi_{\mathrm{S}}(t\mapsto\infty) = H(t) - (1-R)\exp(-t/\tau_{\mathrm{th}}) \tag{9}$$

with R, the ratio of the initial concentration increment to the equilibrium concentration increment:

$$R = \frac{\Delta\varphi_{\mathrm{S}}(t=0^+)}{\Delta\varphi_{\mathrm{S}}(t\mapsto\infty)} = \left(1 - \frac{K_{\mathrm{P}}\xi}{K_{\mathrm{a}}\tau_{\mathrm{th}}}\right). \tag{10}$$

Eqs. (6) and (9) involve the characteristic time constant τ_{th} that is made of two terms (8): the first one is the classical thermal time constant of a system with a capacity $\mathcal{C}$ and a thermal resistance $1/h_{\mathrm{th}}$ that characterizes the exchange between the film and its surroundings. The second one is due to the sorption or desorption phenomenon and describes the coupling between the solvent concentration and the sample temperature. This term depends on latent heat of the solvent. Depending on the sample characteristics and solvent concentration, one of these two terms may be dominant.

As shown by the equations, the solvent volume fraction takes an initial increment at $t=0^+$ and reaches the equilibrium value corresponding to the pressure and temperature of the chamber with the characteristic time τ_{th}. The initial increment is zero if the thermal capacity of the sample is zero and increases with $\mathcal{C}$, which shows that the energy needed to evaporate $\Delta\varphi_{\mathrm{S}}(t=0^+)$ is taken from the internal energy of the sample. In the same way, at $t=0^+$ the temperature of the sample is different from the temperature of the chamber. Later $T(t)$ reaches the chamber temperature T_{a} with the characteristic time τ_{th}. This model was developed in the case of an infinite mass diffusivity and this time constant has nothing to do with the characteristic mass diffusion time that is usually purchased in gravimetric experiments and may distort the interpretation of sorption kinetics if not taken into account.

Previous to the quantitative analysis given in the next section, some general comments can be derived from the model equations: the two parameters that are useful to estimate the importance of the thermal effect are the time constant τ_{th} and R, the ratio of the initial concentration increment to the equilibrium concentration increment. The thermal effect is not sensitive if R is close to one or τ_{th} much smaller than the characteristic mass diffusion time, τ_{d}. On the contrary sorption experiments interpretation becomes impracticable when R is close to zero and τ_{th} much greater than τ_{d}. For other cases (R between 0 and 1, τ_{th} of the same order or greater than τ_{d}) thermal effect has to be taken into account when analyzing the data. Let us note that these two parameters do not depend on the magnitude of the pressure step, so that decreasing ΔP_{V} does not change the thermal effect. The problem is emphasized when the slope of the activity curve versus solvent volume fraction goes to zero. Indeed K_{a} goes to zero too so that τ_{th} and R tend to infinity and zero, respectively. That is why the domain of high solvent concentrations is more difficult to study.

The values of the two parameters R and τ_{th} depend also on the thermal characteristic of the film substrate. When the substrate is thick, τ_{th} is very large but R is close to one, so that thermal effect disappears Eq. (9) reduces to $\Delta\varphi_{\mathrm{S}}(t)/\Delta\varphi_{\mathrm{S}}(t\mapsto\infty) = H(t)$). Indeed, the phase change energy is then taken from the substrate (or given to the substrate) and only very small variation of the temperature is induced as shown by Eq. (6). That is why experiments on thin films laid on quartz microbalance do not show such anomaly, due to the large thickness of the quartz and the good thermal contact between the film and substrate (the film being coated by spin-coating process) [5]. Use of a thick substrate with a good thermal contact between the substrate and the film may then decrease the thermal effect, providing not passing the balance maximum load.

3.2. Example of PIB films on an aluminium substrate

To illustrate quantitatively the above thermal model, numerical and experimental results are presented in the case of a film of PIB/toluene on an aluminium substrate.

3.2.1. Estimation of h_{th}

The heat transfer coefficient, h_{th}, has been estimated using sorption experiments performed at high activity, where the thermal effect was dominant. Indeed for these experiments the characteristic time was found to be proportional to the film thickness, which shows that the weight evolution is not driven by mass diffusion which should give characteristic time proportional to the square of the film thickness. At high activity K_{a} is very small so that the thermal time τ_{th} is dominated by the second term of τ_{th} (cf. Eq. (8)), which is proportional to e_0.

Sorption and desorption steps between 34.1 and 35.6 hPa (i.e. $0.90 \le a \le 0.94$) for a 13 μm film with a thin aluminium substrate (38 μm) were used to perform the estimation. A numerical model solving the three equations of the thermal model (Eqs. (3)–(5)) was developed. Except for h_{th} all the parameters are assumed to be known and the following data have been used (Sigma-Aldrich, [10–13]): $\rho_{\mathrm{al}} = 2800$ kg/m^3, $c_{\mathrm{al}} = 900$ J/(kg K), $\rho_{\mathrm{S}} = 869$ kg/m^3, $c_{\mathrm{S}} = 1700$ J/(kg K), $\rho_{\mathrm{P}} = 920$ kg/m^3, $c_{\mathrm{P}} = 1960$ J/(kg K), $L = 396$ kJ/kg. The interaction parameter χ was calculated from the equilibrium values obtained at the end of the steps and the Antoine formula was used to express the variation of P_{VS0} with the temperature [14]: $\log(P_{\mathrm{VS0}}) = A - B/(T+C)$, with $A = 9.0782$, $B = 1343.9$, $C = -53.77$, P_{VS0} in Pascal and T in Kelvin. Then, h_{th} was obtained by minimizing a quadratic

criterion (distance between experimental weight and calculated weight), with the Levenberg–Marquardt optimization algorithm [15].

The heat transfer coefficient is estimated to 7 W/(m^2 K) and a very good agreement between the thermal model and the weight data used for the estimation is found, as illustrated in Fig. 2(a). With this value of h_{th} the thermal model was used to evaluate the sample temperature $T(t)$ and the activity $a(t)$. Let us note that calculated deviation between the chamber and the sample temperatures, $|T(t)-T_a|$, may reach 0.5 °C (Fig. 2(b)). As a consequence, the pressure step imposed by the regulation system, $\Delta P_V H(t)$, clearly does not lead to the activity step $\Delta P_V H(t)/P_{VS0}(T_a)$ (Fig. 2(c)). Using an approximative value for the mutual diffusion coefficient D_{SP} of 10^{-10} m^2/s, as expected at high solvent concentration, the mass diffusion characteristic time in the conditions of Fig. 2 is $\tau_d \simeq 5$ s, while the thermal time computed with Eq. (8) and used in Fig. 2(a) is $\tau_{th} \simeq 160$ s: the ratio $\tau_{th}/\tau_d \simeq 30$ and $R \simeq 0.11$, which confirms a posteriori that this experiment is dominated by the thermal effect.

To confirm the estimation of h_{th}, two additional tests were performed: first, the estimated $h_{th}=7$ W/(m^2 K) was used to simulate another data corresponding to a 99 μm film in the domain where thermal effect is dominating ($R<0.05$ and $\tau_{th}>\tau_d$). Fig. 3(a) shows the good agreement observed between model and data for two sorption and desorption steps performed between 34.5 and 36.0 hPa (i.e. $0.91 \leq a \leq 0.95$). The same behavior than previously was obtained for the calculated sample temperature and activity (Fig. 3(b) and (c)).

At least, an estimation of h_{th} using a radiative and conductive model to calculate the heat exchanges between the sample and the chamber was performed. Details are given in Annex B. The radiative contribution, which prevails in the experimental configuration, is found to be about 6 W/(m^2 K), close to the estimated value of h_{th}. The difference ($\simeq 1$ W/(m^2 K)) is of the same order of magnitude than a rough estimation of conductive heat transfer in the vapor (cf. Annex B).

The value of h_{th} used in the following is then 7 W/(m^2 K).

3.2.2. Behavior of the two parameters τ_{th} and R

As previously said the magnitude of the thermal effect depends both on the two parameters R and τ_{th}. The effect is negligible only if R is close to one or if τ_{th} is much smaller than τ_d. These parameters depend on the polymer/solvent system (through $\mathcal{C}$, K_P, K_a, ξ), on the chamber environment (through h_{th}) and on the sample thickness and thermal properties (through $\mathcal{C}$, ξ) (Eqs. (8) and (10)). For the chamber described previously and the PIB/toluene system, we now analyze the influence of the sample thickness (aluminium substrate + film). Let us underline that these results may easily be extended to other systems, and that the main conclusions would be the same.

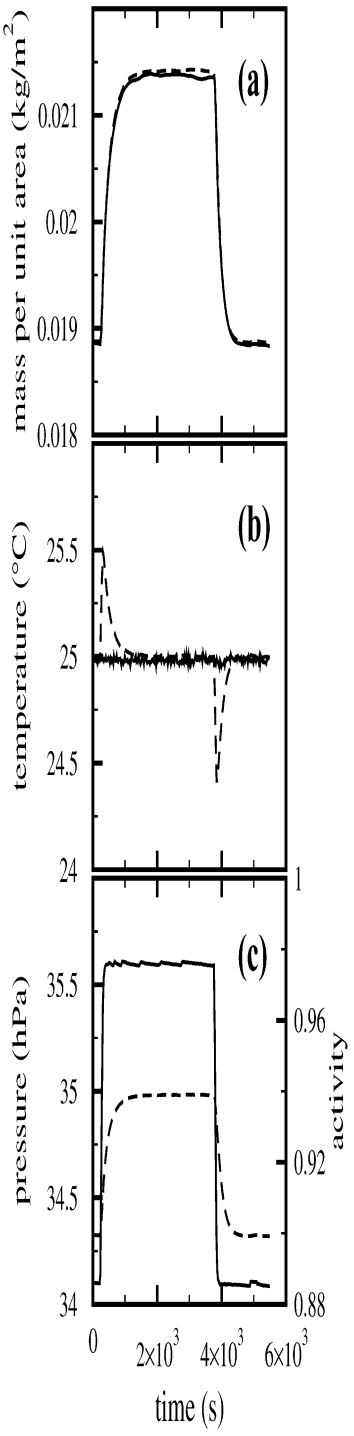

Fig. 2. Estimation of h_{th} with the thermal model—$e_{dry}=13$ μm, $e_{al}=38$ μm. (a) Weight uptake: experimental data (full line) and simulation with the fitted h_{th} value (dashed line). (b) Measured chamber temperature, $T_a(t)$, (full line) and simulated sample temperature (dashed line). (c) Measured pressure $P_V(t)$ (full line) and simulated activity (dashed line).

First the influence of the film substrate on R and τ_{th} is analyzed: Figs. 4 and 5 give the values of the two parameters for a 13 μm film for different substrate thicknesses (3.5 mm, 38 μm and no substrate). The notation 'no substrate' means that the substrate thickness goes to

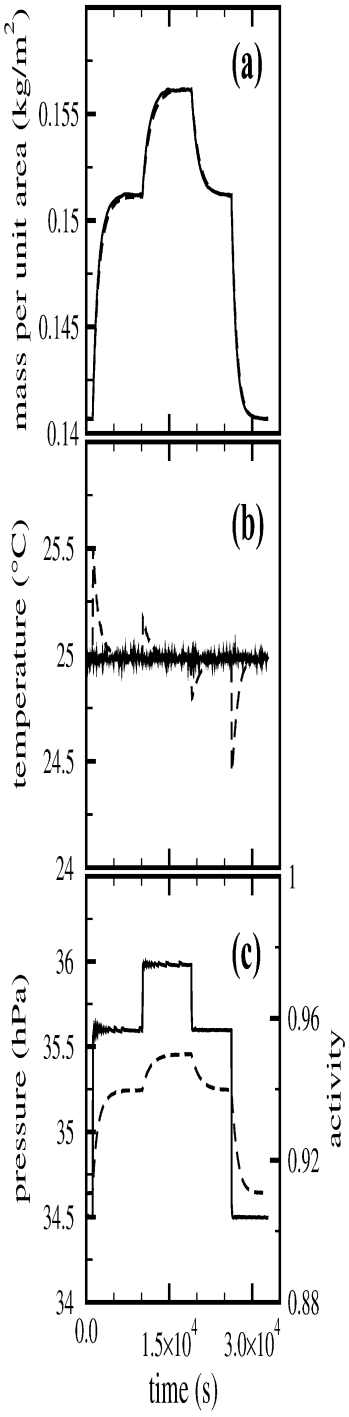

Fig. 3. Comparison between thermal model and experiments—e_{dry} = 99 μm, e_{al} = 38 μm. (a) Weight uptake: experimental data (full line) and simulation with the same h_{th} than in Fig. 2 (dashed line). (b) and (c) Same symbols as in Fig. 2.

zero but that the film is not free, i.e. only one face is in contact with the vapor. Let us note that in the case without substrate, the value of R does not depend on the thickness of the film (cf. Eq. (10) where τ_{th} and ξ are both proportional to e_0). As can be seen, the use of a thick substrate increases the thermal time (by a factor of about 1000 at small solvent

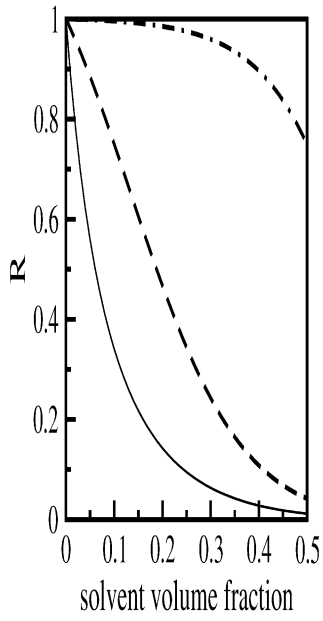

Fig. 4. Results obtained with the linearized thermal model: variation of R with the solvent volume fraction for three aluminium substrate thicknesses: no-substrate (full line), e_{al} = 38 μm (dashed line), e_{al} = 3.5 mm (mixed dashed and dotted line); e_{dry} = 13 μm.

concentration in this example) but leads to high value of R. On the contrary, the case without substrate gives smaller thermal times but R becomes less than 0.5 for a solvent volume fraction of about 0.06.

For a given substrate thickness (38 μm), Figs. 6 and 7 give the evolution of R and τ_{th} for various film thicknesses (e_{dry} = 1, 13, 63, 99 and 1000 μm). The value of R corresponding to very thick film is close to the 'no

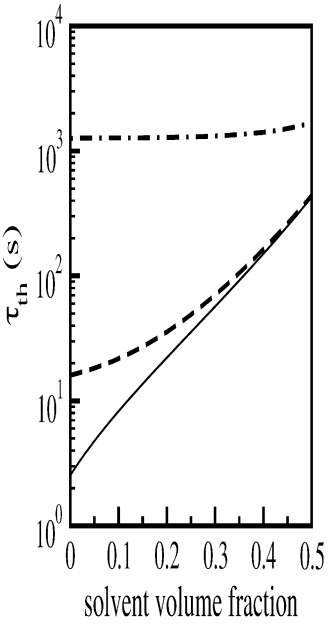

Fig. 5. Results obtained with the linearized thermal model: variation of τ_{th} with the solvent volume fraction for three aluminium substrate thicknesses. Same symbols as in Fig. 4; e_{dry} = 13 μm.

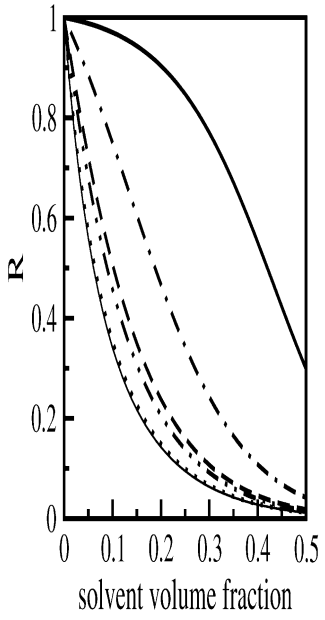

Fig. 6. Results obtained with the linearized thermal model: variation of R with the solvent volume fraction for five film thicknesses: $e_{dry}=1$ μm (thick full line), 13 μm (mixed dotted and dashed line), 63 μm (dashed line), 99 μm (dashed and double dotted line), 1 mm (dotted line), ∞ (thin full line); $e_{al}=38$ μm.

substrate' curve. Indeed, the value of R is the same when $e_{al}=0$ or $e_{dry}\to\infty$. As shown by the figures, R increases and τ_{th} decreases when the film thickness decreases. Let us note that τ_d, the characteristic diffusion time, also decreases, but as the square of the film thickness. The solvent concentration domain where the interpretation of sorption kinetics is affected by the thermal artefact depends on the ratio between τ_{th} and τ_d, and on R, and then on the sample thickness. To illustrate this point and to characterize the domain where the thermal effect may contribute significatively to the sorption kinetics, next section is devoted to the complete analysis of sorption and desorption steps for the 38 μm substrate and three film thicknesses (13, 63, 99 μm).

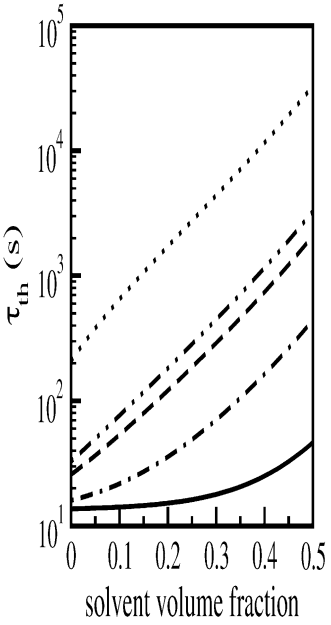

Fig. 7. Results obtained with the linearized thermal model: variation of τ_{th} with the solvent volume fraction for five film thicknesses. Same symbols as in Fig. 6; $e_{al}=38$ μm.

4. Coupling with mutual diffusion

4.1. Model

The previous section was devoted to the analysis of the coupled temperature and solvent concentration, without considering mass diffusion through the film. This section presents the complete model used to analyze sorption and desorption experiments, taking into account mass diffusion through the film and thermal effect [16]. Classical Fickian equation is used in the film, with assumption of constant mutual diffusion coefficient during a differential step

$$\frac{\partial\varphi_S(z,t)}{\partial t}=D_{SP}\frac{\partial^2\varphi_S(z,t)}{\partial z^2},\quad 0<z<e \tag{11}$$

where $\varphi_S(z,t)$ is the local solvent volume fraction. As previously (cf. Section 3.1) the temperature is assumed uniform in the film. The variables of the complete model are $\varphi_S(z,t)$, $e(t)$ and $T(t)$. As in the thermal model the two external input are the pressure in the chamber, $P_V(t)$, and the temperature of the chamber, T_a.

Boundary condition at the film/substrate interface is a non-permeability condition:

$$\frac{\partial\varphi_S}{\partial z}\Big|_{z=0}=0 \tag{12}$$

At the film/vapor interface the boundary condition is given by Eq. (3), where φ_S is the concentration at the interface: $\varphi_S=\varphi_S^i$.

As in the thermal model, two more equations are obtained by writing the heat balance (Eq. (4)) and the non-evaporation of the polymer (Eq. (5)).

For a given D_{SP}, solving Eqs. (3)–(5), (11) and (12) gives the time evolution of the sample temperature $T(t)$, the solvent volume fraction, $\varphi_S(z,t)$, and then the solvent mass in the film. The numerical resolution uses a finite volume discretization, the pure implicit scheme and the Newton–Raphson algorithm.

For each sorption or desorption step, D_{SP} is obtained by minimization of a quadratic criterion comparing the experimental solvent mass evolution and the calculated one on the whole step horizon. Iterative minimization is achieved with the Levenberg–Marquardt algorithm [15].

4.2. Analysis of experimental data

To illustrate the importance of the thermal effect for

various solvent concentrations, we first present the detailed analysis of sorption steps for three solvent concentrations. Comparison is made between the weight data and various models: the thermal model alone presented in the first part of the paper, the complete model described in the previous section and at least the diffusive model usually used in gravimetric data analysis, neglecting the thermal effect: as boundary condition at the upper surface this last model uses the solvent volume fraction given by Eq. (3) with $T=T_a$.

The first example corresponds to a sorption step at small pressure: $0\leq P_V\leq 3$ hPa (that is $0\leq a\leq 0.079$ and $0\leq\varphi_S\leq 0.015$). The thickness of the dry film is 63 μm and the thickness of the aluminium substrate is 38 μm. Experimental data for weight, chamber temperature and chamber pressure are drawn in full lines in Fig. 8. Dashed lines correspond to the thermal model alone: as can be seen thermal characteristic time is very small so that thermal effect does not affect the estimation of the mutual diffusion coefficient. Estimations performed with the complete model (dashed and dotted line) or assuming $T=T_a$ (dotted line) are quite the same and fit very well the experimental weight uptake (Fig. 8(a)). Diffusion coefficient is 1.7×10^{-13} m^2/s and diffusion characteristic time is $\tau_d=23{,}400$ s while $\tau_{th}=30$ s (Fig. 7). As shown in Fig. 6, R is close to one for small solvent volume fraction and the thermal effect is negligible in this concentration domain. The calculated activity is a step function, as the pressure in the chamber (Fig. 8(c)).

For the same sample, the second experiment (Fig. 9) illustrates a situation where thermal and diffusion characteristic times are of the same order: the pressure is varied from 25 to 26 hPa, corresponding to an increase of the activity from 0.66 to 0.69 and of φ_S from 0.179 to 0.193. As shown in Figs. 6 and 7, $R=0.27$ and $\tau_{th}=100$ s, while τ_d estimated with the complete model is 310 s. The complete model (mixed dashed and dotted line) fits very well the experimental data, with a diffusion coefficient $D_{SP}=1.9\times10^{-11}$ m^2/s. (Fig. 9(a)). The dashed curve shows the result of the thermal model alone. The dotted line shows the results obtained when neglecting the thermal effect (with the previously estimated coefficient $D_{SP}=1.9\times10^{-11}$ m^2/s). As can be seen, both contributions (thermal model and solvent diffusion) have to be taken into account to get a correct description of the sorption kinetics. Fig. 9(b) shows the temperature evolution: taking into account mass diffusion decreases the maximum of the temperature deviation compared to the thermal model alone from 0.5 to 0.2 °C. However, a 0.2 °C deviation is enough to introduce a delay in the activity compared to the pressure evolution, as shown in Fig. 9(c). This example is typical of a situation where the complete model is needed to get a correct estimation of D_{SP}. Indeed, the estimation performed with the assumption $T=T_a$ would give a mutual diffusion coefficient two times smaller.

The third example was previously analyzed for the estimation of the heat transfer coefficient, since it is dominated by the thermal effect (cf. Fig. 2, thickness of

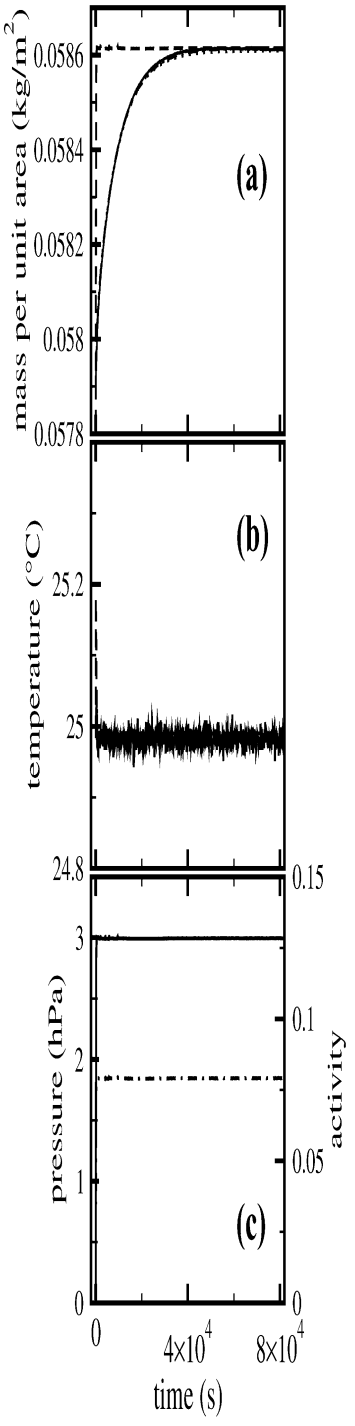

Fig. 8. Sorption step at low pressure—$e_{dry}=63$ μm—$e_{al}=38$ μm: (a) Weight uptake: experimental data (full line), thermal model (dashed line), complete model (mixed dashed and dotted line), diffusion model (dotted line). (b) Measured chamber temperature (full line) and sample temperature simulated with the thermal model (dashed line) and complete model (mixed dashed and dotted line). (c) Measured pressure (full line) and simulated activity (mixed dashed and dotted line).

the dry film = 13 μm, $34.1\leq P_V\leq 35.6$ hPa, $0.90\leq a\leq 0.94$, $0.380\leq\varphi_S\leq 0.455$). Indeed, the diffusion time is very small (a few seconds) and mass diffusion is instantaneous at the time scale of the balance device. The observed weight

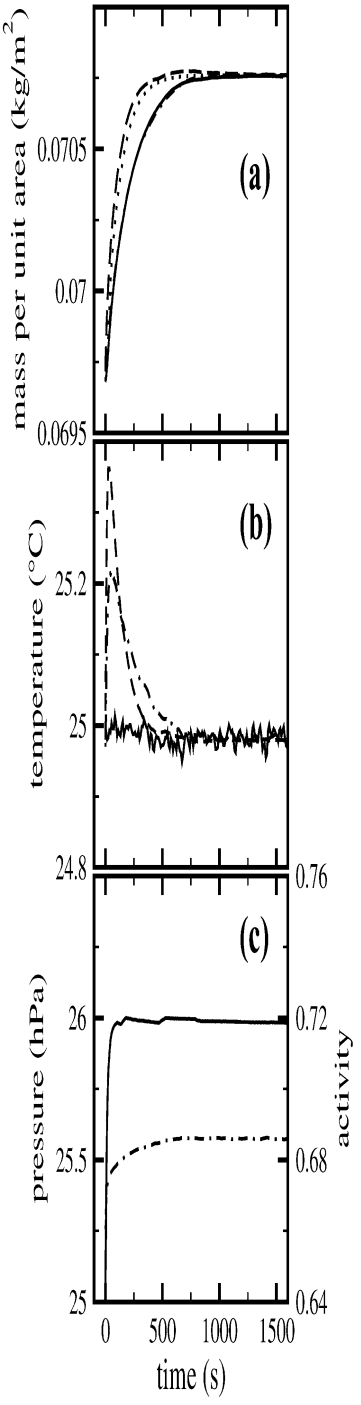

Fig. 9. Sorption step at medium pressure—$e_{dry}=63$ μm—$e_{al}=38$ μm: (a), (b) and (c): Same symbols as in Fig. 8.

evolution during about 500 s is purely due to the variation of the sample temperature.

Given these first results, the complete model was used to analyze all the experimental data obtained for different thicknesses (13, 52, 63 and 99 μm). The thickness of the aluminium substrate is 38 μm. Estimated diffusion coefficients are gathered in Fig. 10. The horizontal error bar corresponds to the solvent volume fraction interval covered

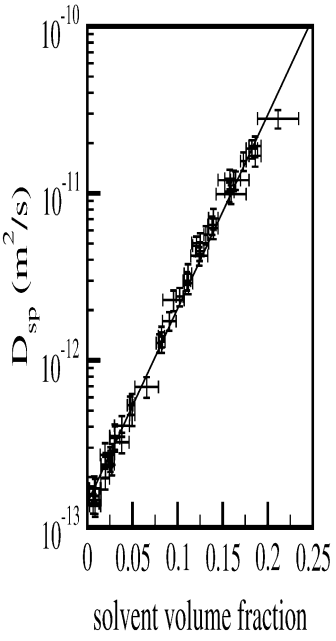

Fig. 10. Mutual diffusion coefficient versus solvent volume fraction for PIB/toluene films [$T_a=25$ °C, dry film thickness = 13, 52, 63 μm ($M_w=5\times10^5$ g/mol) and 99 μm ($M_w=10^6$ g/mol)]. Full line corresponds to an exponential fit.

during the sorption or desorption step. The vertical error bar, that corresponds to the estimation of D_{SP}, is mainly due to the error on the thickness of the dry film: $\Delta D_{SP}/D_{SP}=2\Delta e_{dry}/e_{dry}$, with: $\Delta e_{dry}/e_{dry}=\Delta\bar{V}_S/\bar{V}_S+\Delta S/S+0.1/M_{dry}=6\times10^{-2}+0.1/M_{dry}$ (M_{dry} in mg) where S is the sample surface.

For this polymer/solvent system and with the use of the complete model, estimation of D_{SP} could be accurately performed for $0\leq\varphi_S\leq0.2$. The results for different thicknesses gather on the same curve. A decrease between 3×10^{-11} and 1.4×10^{-13} m²/s when φ_S goes from 0.2 to 0 was found. The data can be well fitted in this concentration domain by: $\log_{10}(D_{SP})=-12.85+11.63\varphi_S$ (D_{SP} in m²/s).

5. Conclusion

Both the numerical results obtained with the analytical thermal model and the analysis of experimental sorption data show the necessity to take into account the film temperature evolution of the sample when fitting experimental kinetics obtained by gravimetry for high activities. Indeed a small change in the sample temperature induces a change in the surface solvent concentration that can be significant compared to the solvent concentration change during the sorption. If the thermal and mass characteristic times are also of the same order of magnitude, a pressure step no more induces a surface concentration step and this thermal effect must be taken into account. A first analysis (pure thermal model) gives a rough estimation of the solvent concentration domain where thermal effect may interfere

with mass diffusion. In practice, for a given system, the choice of the suitable film and substrate thicknesses depends on a compromise between the balance limitations, a 'reasonable' (not too long) experimental time and the minimization of the thermal effect described in this paper.

A complete model was then developed and applied to sorption and desorption steps on the system PIB/toluene. Accurate estimation of the mutual diffusion coefficient was obtained for solvent volume fraction up to 0.2.

Annex A. Thermal model

The thermal model uses the assumption of an infinite mass diffusion coefficient in the film. The two external input of the system are the pressure in the chamber, $P_V(t)$, and the temperature of the chamber, $T_a(t)$, both imposed by the regulation system. The unknown variables are $\varphi_S(t)$, $T(t)$ and the film thickness $e(t)$, whose time evolution are derived from the three Eqs. (3)–(5).

In the case of differential sorption experiments, the expression of $P_{VS}(\varphi_S,T)$ can be derived from a first order development:

$$P_{VS}(T,\varphi_S) \simeq P_{VS}(T_0,\varphi_{S0}) + \left.\frac{\partial P_{VS}}{\partial T}\right|_{T_0,\varphi_{S0}} dT + \left.\frac{\partial P_{VS}}{\partial \varphi_S}\right|_{T_0,\varphi_{S0}} d\varphi_S$$

$$= P_{VS}(T_0,\varphi_{S0}) + a(\varphi_{S0})\left.\frac{dP_{VS0}}{dT}\right|_{T_0} dT + P_{VS0}(T_0)\left.\frac{da}{d\varphi_S}\right|_{\varphi_{S0}} d\varphi_S$$

That gives

$$\frac{d\varphi_S}{dt} = \frac{1}{K_\varphi}\frac{dP_V}{dt} - \frac{K_P}{K_a}\frac{dT}{dt}$$

with:

$$K_\varphi = P_{VS0}(T_0)\left.\frac{da}{d\varphi_S}\right|_{\varphi_{S0}}, \qquad K_a = \frac{1}{a(\varphi_{S0})}\left.\frac{da}{d\varphi_S}\right|_{\varphi_{S0}}, \quad K_P = \frac{1}{P_{VS0}(T_0)}\left.\frac{dP_{VS0}}{dT}\right|_{T_0} \tag{A.1}$$

The term $d(e\varphi_S)/dt$ in the heat balance equation is written in the following way:

$$\frac{d(e\varphi_S)}{dt} = \varphi_S\frac{de}{dt} + e\frac{d(\varphi_S)}{dt}$$

This last equation together with Eq. (5) give

$$\frac{d(e\varphi_S)}{dt} = \frac{e}{(1-\varphi_S)}\frac{d(\varphi_S)}{dt}$$

that is approximated by:

$$\frac{d(e\varphi_S)}{dt} \simeq \frac{e_0}{(1-\varphi_{S0})}\frac{d(\varphi_S)}{dt}$$

Using the expression of $d\varphi_S/dt$ derived from Eq. (3), the above approximation and the heat balance lead to:

$$\tau_{th}\frac{dT}{dt} = (T_a - T) + \frac{\xi}{K_\varphi}\frac{dP_V}{dt} \tag{A.2}$$

with:

$$\xi = \frac{Le_0}{h_{th}\bar{V}_S(1-\varphi_{S0})}, \quad \tau_{th} = \frac{C}{h_{th}} + \frac{K_P}{K_a}\xi$$

In the case of a pressure differential step, $P_V(t) = \Delta P_V H(t)$ and $dP_V/dt = \Delta P_V \delta(t)$ where $H(t)$ and $\delta(t)$ are the Heaviside and delta functions, respectively. The expression of $T(t)$ is easily derived by use of Laplace transform:

$$\Delta T(t) = T(t) - T_a = \frac{\xi \Delta P_V}{K_\varphi \tau_{th}}\exp(-t/\tau_{th})$$

The expression of φ_S is obtained in the same way:

$$\Delta\varphi_S(t) = \varphi_S - \varphi_{S0} = \frac{\Delta P_V}{K_\varphi}\left[H(t) - \frac{K_P\xi}{K_a\tau_{th}}\exp(-t/\tau_{th})\right]$$

Annex B. Estimation of h_{th}

B.1. Radiative flux

The estimation of the radiative flux is made with the assumption of a small sample compared to the chamber size.

The sample is made of the aluminium substrate, with total hemispheric emissivity ε_{al}, and of the polymer film, with total hemispherical emissivity ε_{film}.

Radiative flux may be expressed as [10]:

$$\phi_{film}^{rad} = \varepsilon_{film} S\sigma(T^4 - T_a^4) \simeq 4\varepsilon_{film} S\sigma T_a^3 (T - T_a) \tag{B.1}$$

and

$$\phi_{al}^{rad} = \varepsilon_{al} S\sigma(T^4 - T_a^4) \simeq 4\varepsilon_{al} S\sigma T_a^3 (T - T_a) \tag{B.2}$$

then

$$\phi^{rad} = \phi_{al}^{rad} + \phi_{film}^{rad} = h^{rad} S(T - T_a)$$

with:

$$h^{rad} = 4(\varepsilon_{film} + \varepsilon_{al})\sigma T_a^3$$

Total hemispherical emissivity for aluminium at 27 °C is between 0.04 and 0.082, depending of the state of the surface. Total hemispherical emissivity for a classical rubber is about 0.92 at 20 °C [17,10].

Using overestimation and underestimation of the two emissivities, one gets: $5\ W/(m^2\ K) \le h^{rad} \le 6.5\ W/(m^2\ K)$.

B.2. Conductive flux

To get the order of magnitude of the conductive contribution, h^{cond} is estimated by $h^{cond} \sim \lambda/L$ where λ is the thermal conductivity of the solvent vapor

($\sim$0.01 W/(m K)) and L the chamber radius (17.5 mm), that is: $h^{cond} \sim 1$ W/(m^2 K).

References

[1] Stamatialis D, Wessling M, Sanopoulou M, Strathmann H, Petropoulos J. J Membr Sci 1997;125:165–75.
[2] Billovits G, Durning C. Macromolecules 1994;27:7630–44.
[3] Huang S, Durning C. J Polym Sci B 1997;35:2103–19.
[4] Sanopoulou M, Petropoulos J. Polymer 1997;23:5761–8.
[5] Dubreuil A-C, Doumenc F, Guerrier B, Johannsmann D, Allain C. Polymer 2003;44:377–87.
[6] Dubreuil A-C, Doumenc F, Guerrier B, Allain C. Macromolecules 2003;36:5157–64.
[7] Armstrong A, Wellons J, Stannett V. Die Makromol Chem 1966;95: 78–91.
[8] Saeki S, Tsubokawa M, Yamaguchi T. Macromolecules 1987;20: 2930–4.
[9] Petri H, Wolf B. Macromol Chem Phys 1995;196:2321–33.
[10] Incropera F, DeWitt D. Introduction to heat transfer. London: Wiley; 1996.
[11] Weast RC, AStle MJ. Handbook of chemistry and physics; 61st ed. Boca Raton: CRC Press; 1980.
[12] Chow T. Macromolecules 1980;13:362–4.
[13] Brandrup J, Immergut E. Polymer handbook. New York: Wiley Interscience; 1989.
[14] Riddick J, Bunger W. Techniques of chemistry: vol. II, organic solvents, physical properties and methods of purification. 3rd ed. New York: Wiley-Interscience; 1970.
[15] Walter E, Pronzato L. Identification of parametric models from experimental data. Berlin: Springer; 1997.
[16] Guerrier B, Bouchard C, Allain C, Benard C. J AIChE 1998;44(4): 791–8.
[17] Sacadura(Coordonnateur) J-F. Initation aux transferts thermiques; Lavoisier; 1993.